Carcinogenesis vol.33 no.4 pp.848–858, 2012
doi:10.1093/carcin/bgs019
Advance Access publication January 19, 2012

Generation of reactive oxygen species by grape seed extract causes irreparable DNA damage leading to G_2/M arrest and apoptosis selectively in head and neck squamous cell carcinoma cells

Sangeeta Shrotriya[1], Gagan Deep[1,2], Mallikarjuna Gu[1], Manjinder Kaur[1], Anil K.Jain[1], Swetha Inturi[1], Rajesh Agarwal[1,2] and Chapla Agarwal[1,2,*]

[1]Department of Pharmaceutical Sciences, Skaggs School of Pharmacy and Pharmaceutical Sciences, University of Colorado, Aurora, CO 80045, USA and [2]University of Colorado Cancer Center, Aurora, CO 80045, USA

[*]To whom correspondence should be addressed. Room V20-2118, Box C238, Department of Pharmaceutical Sciences, Skaggs School of Pharmacy and Pharmaceutical Sciences, University of Colorado, 12850 E. Montview Boulevard, Aurora, CO 80045, USA. Tel: +1 303 724 4057;
Fax: +1 303 724 7266;
Email: Chapla.Agarwal@UCDenver.edu
Correspondence may also be addressed to Rajesh Agarwal.
Tel: +1 303 724 4057; Fax: +1 303 724 7266;
Email: Rajesh.Agarwal@ucdenver.edu

Head and neck squamous cell carcinoma (HNSCC) accounts for 6% of all malignancies in USA and unfortunately the recurrence of secondary primary tumors and resistance against conventional treatments decrease the overall 5 year survival rate in HNSCC patients. Thus, additional approaches are needed to control HNSCC. Here, for the first time, employing human HNSCC Detroit 562 and FaDu cells as well as normal human epidermal keratinocytes, we investigate grape seed extract (GSE) efficacy and associated mechanism in both cell culture and nude mice xenografts. GSE selectively inhibited the growth and caused cell cycle arrest and apoptotic death in both Detroit 562 and FaDu cells by activating DNA damage checkpoint cascade, including ataxia telangiectasia mutated/ataxia telangiectasia-Rad3-related–checkpoint kinase 1/2–cell division cycle 25C as well as caspases 8, 9 and 3. Consistent with these results, GSE treatment resulted in a strong DNA damage and a decrease in the levels of DNA repair molecules breast cancer gene 1 and Rad51 and DNA repair foci. GSE-caused accumulation of intracellular reactive oxygen species was identified as a major mechanism of its effect for growth inhibition, DNA damage and apoptosis, which was remarkably reversed by antioxidant *N*-acetylcysteine. GSE feeding to nude mice decreased Detroit 562 and FaDu xenograft tumor growth by 67 and 65% ($P < 0.001$), respectively. In immunohistochemical analysis, xenografts from GSE-fed groups showed decreased proliferation but increased DNA damage and apoptosis. Together, these findings show that GSE targets both DNA damage and repair and provide mechanistic insights for its efficacy selectively against HNSCC both in cell culture and mouse xenograft, supporting its translational potential against HNSCC.

Introduction

Head and neck squamous cell carcinoma (HNSCC) accounts for one of the leading malignancies in the USA with >49 000 new cases and 11 000 HNSCC-associated deaths only in last year 2010 (1). Radiation and chemotherapy are the conventional treatment options available for HNSCC patients at both early and late stage of the malignancy; unfortunately, the patients with HNSCC are generally diagnosed at an advanced stage of the disease (2–4). Furthermore, the recurrence of secondary primary tumors and the development of resistance against conventional treatments decrease the overall 5 year survival rate in HNSCC patients (5,6). These grim figures and limitations associated with HNSCC treatment and control suggest that additional approaches and strategies are needed with non-toxic agents for the prevention/intervention of both primary HNSCC and the recurrence of secondary primary tumors post-HNSCC therapy. One such class of non-toxic agents is polyphenolic phytochemicals present in diet or those consumed as supplements (7,8). In this context, various epidemiological studies and animal experiments have shown that consumption of vegetable- and fruit-based diet remarkably reduces the overall risk of cancer (9–11). Accordingly, several preclinical and clinical studies have also focused on the identification of non-toxic phytochemicals and validating their efficacy against various malignancies (12).

One of the phytochemicals extensively investigated in recent years is grape seed extract (GSE), which is a defined mixture of gallic acid, catechin, epicatechin and proanthocyanidins (8,13,14). Potent anticancer efficacy of GSE has been reported against several malignancies in both *in vitro* and *in vivo* studies (15,16). The pharmacological and translational significance of GSE lies in its frequent consumption as a dietary supplement for various health benefits without any known toxicity or untoward effects in humans (17,18). Previous studies have shown growth inhibition of oral tumor cell lines by GSE (19,20); however, the detailed *in vitro* and *in vivo* biological efficacy, the selectivity and the underlying primary molecular mechanism of GSE against human HNSCC cell lines are largely unknown. Accordingly, this was the focus of the present study. Our results show that GSE treatment induces accumulation of intracellular reactive oxygen species (ROS) in HNSCC cells leading to DNA damage, and that GSE simultaneously decreases DNA damage repair molecules; thereby, making the DNA damage irreparable. These actions of GSE cause a cell cycle arrest in G_2/M phase together with cell growth inhibition and apoptotic cell death both in cell culture and nude mice xenografts of human HNSCC Detroit 562 and FaDu cells.

Abbreviations: ATM, ataxia telangiectasia mutated; ATR, ataxia telangiectasia-Rad3-related; Brca1, breast cancer gene 1; Cdc25C, cell division cycle 25C; Chk, checkpoint kinase; DCF-DA, 2′,7′-dichlorofluorescein diacetate; DHE, dihydroeithidium; DSB, double-strand break; GSE, grape seed extract; HNSCC, head and neck squamous cell carcinoma; HRR, homologous recombination repair; IHC, immunohistochemistry; NAC, N-acetylcysteine; NHEJ, non-homologous end joining; PCNA, proliferating cell nuclear antigen; ROS, reactive oxygen species; PARP, poly (adenosine diphosphate ribose) polymerase; TUNEL, terminal deoxynucleotidyl transferase-mediateddeoxyuridine triphosphatenick end labeling.

Materials and methods

Cell lines and reagents

HNSCC Detroit 562 and FaDu cells were from American type culture collection (Manassas, VA) and cultured in Dulbecco's modified Eagle's medium under standard conditions. Normal human epidermal keratinocytes were cultured in Clonetics™ KGM-Gold™ medium along with essential supplements provided by Lonza (Walkersville, MD). GSE used in this study was from San Joaquin Valley Concentrates (Fresno, CA) and sold as ActiVin, which is highly rich in oligomeric proanthocyandins and other valuable flavonoids as reported earlier (21). Antibodies for cyclin B1, phospho-cell division cycle 25C (Cdc25C) (Ser216), Cdc25C, checkpoint kinase 1/2 (Chk1/2) and Rad51 were from Santa Cruz Biotechnology (Santa Cruz, CA); for cleaved caspase-3, -9, -8 and cleaved poly (adenosine diphosphate ribose) polymerases (PARP), phospho-Chk1 (Ser296 and Ser345), phospho-Chk2 (Thr68), phospho-H2A.X (Ser139), phospho-Cdc2 (Tyr15), Cdc2, breast cancer gene 1 (Brca1), Mre11, Nbs1 and secondary anti-rabbit antibody were from Cell Signaling (Beverly, MA); anti-Rad50 was from Abcam (Cambridge, UK); phospho-ataxia telangiectasia mutated (ATM) (Ser1981) was from Rockland Immunochemicals (Gilbertsville, PA) and for phospho-ataxia telangiectasia-Rad3-related (ATR) (Ser428) was from Novus Biological (Littleton, CO). Secondary anti-mouse antibody and Enhanced chemiluminescence system were from GE. β-Actin antibody and 2′,7′-dichlorofluorescein diacetate (DCF-DA) were from Sigma–Aldrich (St Louis, MO). Dihydroeithidium (DHE) was from Invitrogen (Carlsbad, CA). Proliferating cell nuclear antigen

(PCNA) antibody, streptavidin and biotinylated anti-mouse secondary antibody were from Dako (Carpinteria, CA), and Terminal Deoxynucleotidyl Transferase-Mediated Deoxyuridine Triphosphate Nick End Labeling (TUNEL) assay kit was from Promega (Madison, MI).

Cell viability, cell cycle and quantitative apoptosis assays

Cells were plated at 5000/cm^2 density and after 24 h, fed with fresh medium containing either dimethyl sulfoxide or GSE in dimethyl sulfoxide (20 and 40 μg/ml concentrations). At various time-points, cells were collected by brief trypsinization and cell number and death determined by trypan blue exclusion assay using hemocytometer. In other experiments, Detroit 562 and FaDu cells were pretreated with 5 and 15 mM N-acetylcysteine (NAC) (after standardizing NAC concentration in both cell lines), respectively, for 15 min prior to GSE treatment and cell viability was measured at desired time-point. GSE effect on cell cycle progression of HNSCC cells was assessed by fluorescence-activated cell sorting analysis following earlier published method (22). Induction of apoptosis in GSE-treated HNSCC cells was determined using Vybrant Apoptosis Assay Kit 2 following vendor's protocol (Molecular Probes, Eugene, OR).

Western blotting

Whole cell lysates were prepared from dimethyl sulfoxide- or GSE-treated cells and western blotting was performed following earlier described methods (22). To ensure equal protein loading, each membrane was stripped and reprobed with anti-β-actin antibody, which was also used in densitometric analyses of immunoblots to normalize for differences in protein loading.

Comet assay

GSE-induced DNA damage was analyzed by a single cell gel electrophoresis (comet assay) as detailed earlier (23). The slides were stained with propidium iodide, dried and observed under Nikon inverted microscope (Nikon, Japan). Images were captured using CoolSNAP$_{ES}$ charge-coupled device camera attached to the microscope and the extent of DNA damage was measured using Komet 5.5 software (ANDOR Technology, South Windsor, CT). Next, percent DNA in comet tail was calculated from tail extent moment, which correlates with the level of DNA damage.

Immunofluroscence assay

Phospho-H2A.X (Ser139), Brca1 and Rad51 cellular levels and localization were also analyzed by immunoflorescence following the protocol described earlier (24). Images were captured at ×600 magnification on a Nikon inverted confocal microscope using 488/402 nm laser wavelengths to detect fluorescein isothiocyanate (green) and 4′,6′-diamidino-2-phenylindole (blue) emissions, respectively.

ROS measurement

DCF-DA and DHE were used to examine GSE effect on intracellular ROS (both H_2O_2 and superoxide) generation. For DCF-DA staining, cells were cultured, washed with Krebs-ringer bicarbonate solution and incubated with 20 μM freshly prepared DCF-DA solution in dark. After 30 min, DCF-DA was removed and cells were washed with Krebs-ringer bicarbonate solution, followed by incubation with 40 μg/ml of GSE. Finally, the fluorescence was measured at different time-points using Spectramax Gemini^{EM} fluorescence plate reader (Molecular Devices, Sunnyvale, CA) with excitation filter set at 485 nM and emission filter set at 530 nM. For DHE staining, cells were treated with GSE (40 μg/ml) followed by incubation with 10 μM DHE and analyzed for fluorescence intensity by flow cytometry. The results were obtained by gating the DHE fluorescence versus linear side scatter (SS Lin) of cells. In another study, HNSCC cells were pretreated with NAC for 15 min followed by GSE (40 μg/ml) treatment and ROS levels were measured as described above for both DCF-DA and DHE staining.

In vivo *tumor xenograft study*

Six-week-old athymic nu/nu male mice were obtained from the National Cancer Institute (Bethesda, MD) and were housed in an animal care facility at standard laboratory conditions, following the protocols approved by the Institutional Animal Care and Use Committee (IACUC) of University of Colorado Denver. HNSCC cells namely, Detroit 562 and FaDu were harvested by brief trypsinization, washed twice and resuspended in serum-free Dulbecco's modified Eagle's medium. The animals were divided into two groups (16 animals each group), and Detroit 562 cells (∼5 million) or FaDu cells (∼2 million) were mixed with 50 μl of matrigel and injected subcutaneously on the right flank of each mouse in Group 1 or 2, respectively, as described before (25). A week after cell injection, mice in both groups were randomly divided into two subgroups; control subgroup mice were fed with regular AIN-76A diet (Dyets, Bethlehem, PA) and treatment subgroup mice were fed with 0.2% GSE (wt/wt) in diet. The GSE dose selection for the present study was based on our earlier published observation, where GSE was effective and well tolerated by mice (26). Animals were evaluated twice weekly for body weight, diet consumption and tumor growth. Tumor volume was determined using the formula $0.5236L_1(L_2)^2$, where L_1 and L_2 are the long and short axes of the tumor dimension, respectively. At the end of the experiment, animals were euthanized and tumors were removed and weighed; a part of each tumor was fixed in buffered formalin for immunohistochemical (IHC) analysis and the rest stored at −80°C.

IHC analysis

Formalin-fixed tumor samples were paraffin-embedded and used for IHC analyses of PCNA and phospho-H2A.X (Ser139) following the earlier described methods (25). The apoptotic cell population in the tumor sections was determined by DeadEnd Colorimetric TUNEL assay kit (Promega, Madison, WI). The percent positive stained cells were determined as number of positive cells (brown stained) × 100/total number of cells in five randomly selected area per tumor section at ×400 magnification, and images were processed by Zeiss AxioVision software documentation system (Carl Zeiss, Jena, Germany).

Statistical analysis

Statistical analysis was performed using SigmaStat 2.03 software (Jandel Scientific, San Rafael, CA). Immunoblots were scanned using Adobe Photoshop 6.0 (Adobe system, San Jose, CA), and band intensity was measured using Scion Image program (National Institutes of Health, Bethesda, MD). Data were analyzed using analysis of variance and a statistically significant difference was considered at $P < 0.05$.

Results

GSE strongly inhibits growth and causes G_2/M arrest and apoptotic death of HNSCC cells

As shown in Figure 1A, GSE treatment strongly decreased live cells number and caused cell death in a dose- and time-dependent manner in both Detroit 562 and FaDu cells. The live cell number decreased by 10–30% ($P < 0.05$–0.001) and 18–70% ($P < 0.05$–0.001) in Detroit 562 cells and 15–84% ($P < 0.001$) and 25–90% ($P < 0.05$–0.001) in FaDu cells following GSE treatment (12–72 h) at 20 and 40 μg/ml doses, respectively (Figure 1A). Similarly, GSE treatment (12–72 h) increased percent cell death by 5–24% ($P < 0.05$–0.001) and 8–50% ($P < 0.05$–0.001) compared with control in Detroit 562 cells and 6–34% ($P < 0.05$–$P < 0.001$) and 9–40% ($P < 0.05$–$P < 0.001$) in FaDu cells at 20 and 40 μg/ml doses, respectively (Figure 1A). Importantly, similar GSE concentrations (20 and 40 μg/ml) did not affect the total cell number and only marginally decreased the live cell number of normal human epidermal keratinocytes after 48 and 72 h, with no GSE effect after 24 h (Figure 1B). This data showed GSE selectivity toward HNSCC cells only.

To gain insight into growth inhibitory and death effects of GSE, we next assessed its effect on cell cycle progression and apoptosis induction. In both Detroit 562 and FaDu cells, GSE treatment resulted in a significant accumulation of cells in G_2/M phase, at the expense of a decrease in both G_1 and S phase cell populations. In comparison with control (∼17% of G_2/M population), GSE treatment (24 and 48 h) resulted in G_2/M accumulation by 20–25% ($P < 0.05$–0.001) and 26–35% ($P < 0.001$–$P < 0.001$) in Detroit 562 cells and 53–41% ($P < 0.001$–$P < 0.001$) and 54–44% ($P < 0.001$–$P < 0.001$) in FaDu cells at 20 and 40 μg/ml doses, respectively (Figure 1C). The GSE-caused G_2/M arrest was very profound even at lower dose and shorter treatment time in FaDu cells compared with Detroit 562 (Figure 1C). GSE treatment also significantly induced apoptotic cell death in both HNSCC cell lines mostly in a dose-dependent manner. As shown in Figure 1D, with GSE treatment (24–72 h) apoptotic cell population was 11–15% ($P < 0.05$–$P < 0.001$) and 27–42% ($P < 0.001$–$P < 0.001$) in Detroit 562 cells and 25–14% ($P < 0.05$–$P < 0.001$) and 38–48% ($P < 0.001$–$P < 0.001$) in FaDu cells at 20 and 40 μg/ml doses compared with ∼7 and ∼3% in controls, respectively (Figure 1D). Together, these results convincingly demonstrate that GSE possess strong growth inhibitory and cell death effects in HNSCC cells.

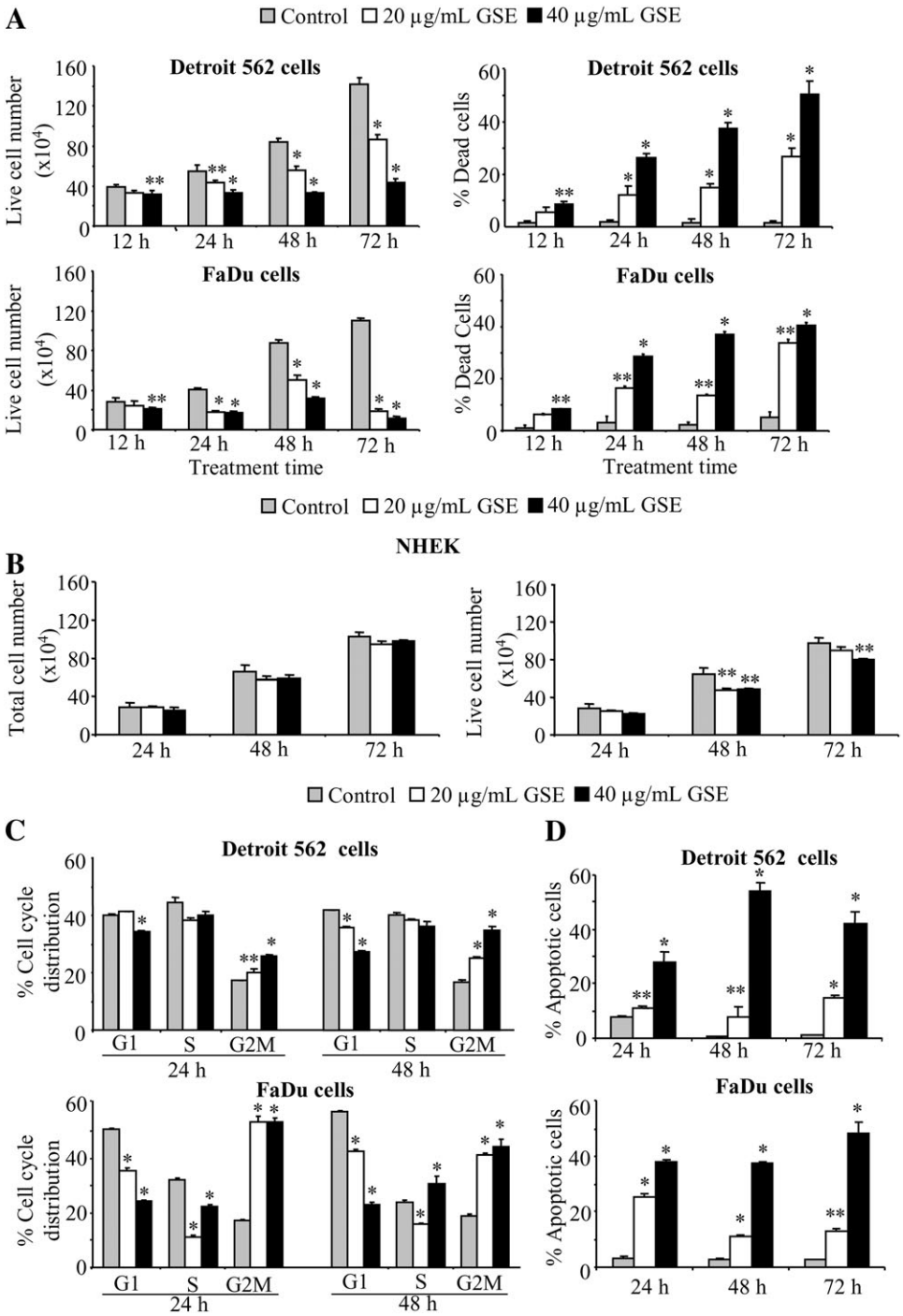

Fig. 1. Effect of GSE on growth, death and cell cycle distribution in HNSCC and normal human epidermal keratinocytes (NHEK) cells. Detroit 562, FaDu and NHEK cells were treated with either dimethyl sulfoxide or different concentrations of GSE (20 and 40 µg/ml) for 12–72 h. Thereafter, cells were collected and processed as detailed in 'Materials and methods' to analyze GSE effects on (**A**) live and dead HNSCC cell number, (**B**) total and live NHEK cell number, (**C**) cell cycle distribution and (**D**) apoptosis. Each bar is a representative of mean ± SEM of three samples for each treatment. $^{*}P < 0.001$; $^{**}P < 0.05$.

GSE activates DNA damage sensor kinases and associated cellular checkpoints as well as caspases in HNSCC cells

In the studies examining mechanism of G_2/M arrest, GSE treatment strongly increased the phosphorylation of DNA damage sensor kinases ATM (at Ser1981) and ATR (at Ser428) in both Detroit 562 and FaDu cells, starting 6 h of its treatment that remained elevated at 72 h of study time-point (Figure 2A and 2B). These results corroborated with downstream effectors showing the activation of cellular Chk2 (Thr68) and Chk1 (Ser296 and Ser345), which are known to control cell cycle through inactivating phosphorylation of Cdc25 (27), without any noticeable change in total Chk2 and Chk1 levels (Figure 2A and 2B). Consistently, GSE also increased the phosphorylation of Cdc25C at Ser216 site without affecting its total level except at later time-points in FaDu cells (Figure 2A and 2B). Cdc25C phosphatase in particular regulates the activity of Cdc2/cyclin B1, a rate-limiting complex for cells to enter mitosis (28). Whereas GSE did not affect phospho-Cdc2 (Tyr15) and total Cdc2 levels (data not shown), it strongly decreased cyclin B1 level in both the cell lines (Figure 2A and

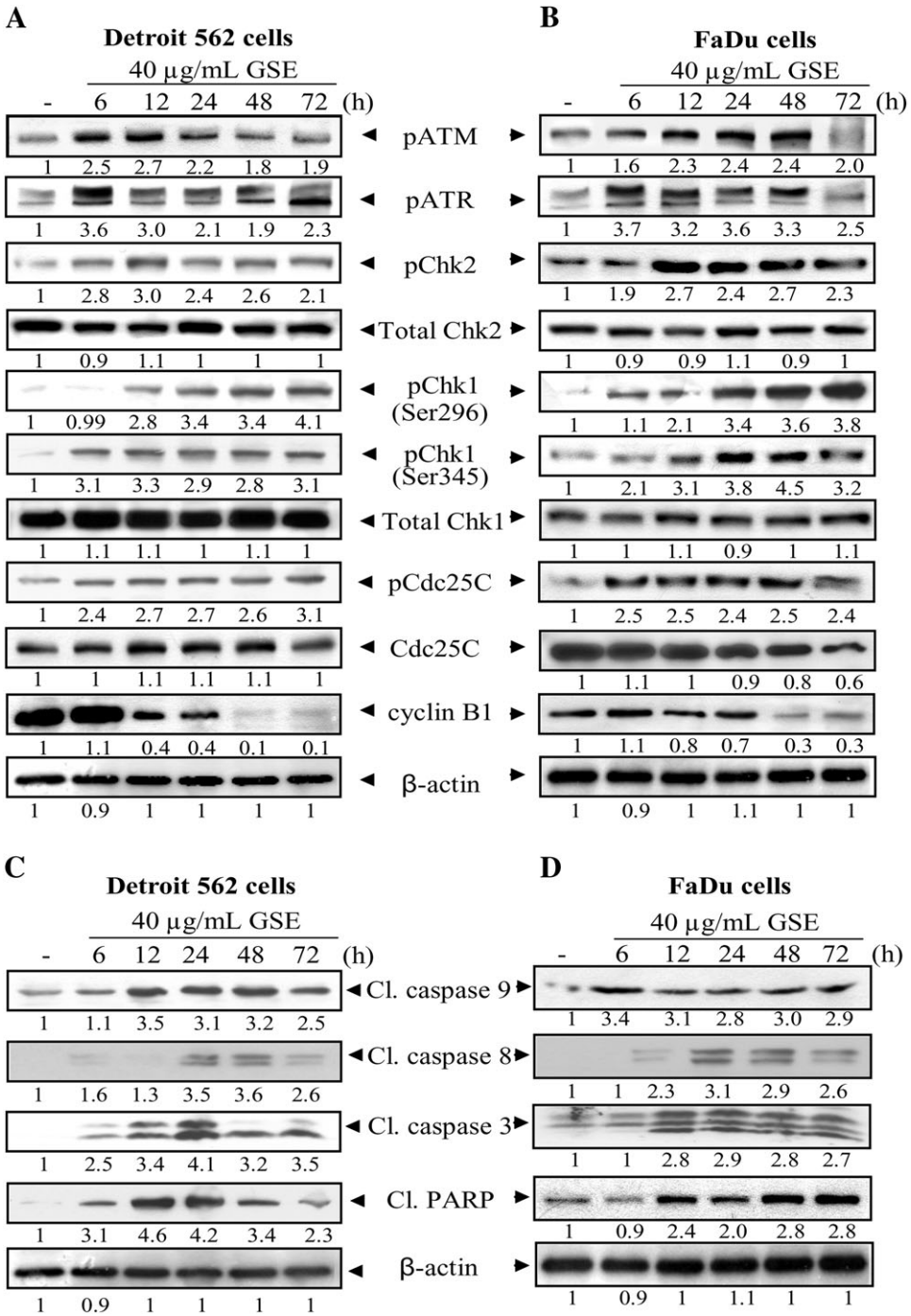

Fig. 2. Effect of GSE on the expression of DNA damage sensors, checkpoint signaling and apoptosis in HNSCC cells. Detroit 562 and FaDu cells were treated with GSE (40 μg/ml) for 6–72 h, and total cell lysates were prepared and subjected to sodium dodecyl sulfate–polyacrylamide gel electrophoresis and western blotting. The membranes were then analyzed for (**A** and **B**) DNA damage sensors, Chks and cell cycle regulators, and (**C** and **D**) cleaved caspases and PARP levels. Equal protein loading was confirmed by reprobing the membrane with β-actin. The densitometry data below the bands represents 'fold change' as compared with vehicle control after normalization with respective loading control.

2B). Together, these results suggest that GSE treatment activates DNA damage sensor kinases and associated cellular checkpoints causing G_2/M arrest in HNSCC cells.

The major mechanism of apoptotic cell death is via activation of extrinsic (caspase 8) and/or intrinsic (caspase 9) pathways ultimately activating caspase 3 and PARP cleavage causing apoptotic cell death (29). In the present studies assessing whether caspases are involved in observed apoptotic death, GSE treatment (40 μg/ml) caused a strong and time-dependent activation of both intrinsic and extrinsic pathways as evidenced by cleaved caspase 9 and caspase 8 levels as well as those of cleaved caspase 3 and PARP (Figure 2C and 2D), suggesting the involvement of both these pathways in GSE-caused apoptotic death in HNSCC cell lines.

GSE causes DNA damage and decreases the level of repair enzymes in HNSCC cells

H2A.X is critical for facilitating the assembly of specific DNA repair complexes on damaged DNA site (30). In response to DNA double-strand break (DSB), H2A.X is recruited at the site of DSB and gets phosphorylated at Ser139 site by various kinases, including ATM,

ATR and DNA-dependent protein kinase, allowing it to accumulate at the site of DNA damage (31). Based on our results showing that GSE activates both ATM and ATR, next we assessed its effect on DNA damage in both Detroit 562 and FaDu cells. As shown in Figure 3A, GSE caused a strong H2A.X phosphorylation as early as 6 h post-treatment in both cell lines, which persisted till 72 h. Next, we confirmed the GSE-induced DNA damage in HNSCC cells using comet assay, which also showed a strong DNA-damaging effect of GSE in both HNSCC cell lines as indicated by tail extent moment (Figure 3B).

Based on the results showing that GSE causes DNA damage in both HNSCC cell lines, the next logical question was to determine whether GSE-induced DNA damage was repairable by assessing the expression of enzymes involved in DNA repair. Notably, the repair of DSBs involves localization of DNA repair enzymes at the site of DNA damage via two major processes, including homologous recombination repair (HRR) and non-homologous end joining (NHEJ) (30). As shown in Figure 3C, GSE treatment for 24 and 48 h also caused a decrease in the protein levels of Brca1 and Rad51; the DNA repair enzymes involved in NHEJ and HRR (30,31), in concentration-dependent manner

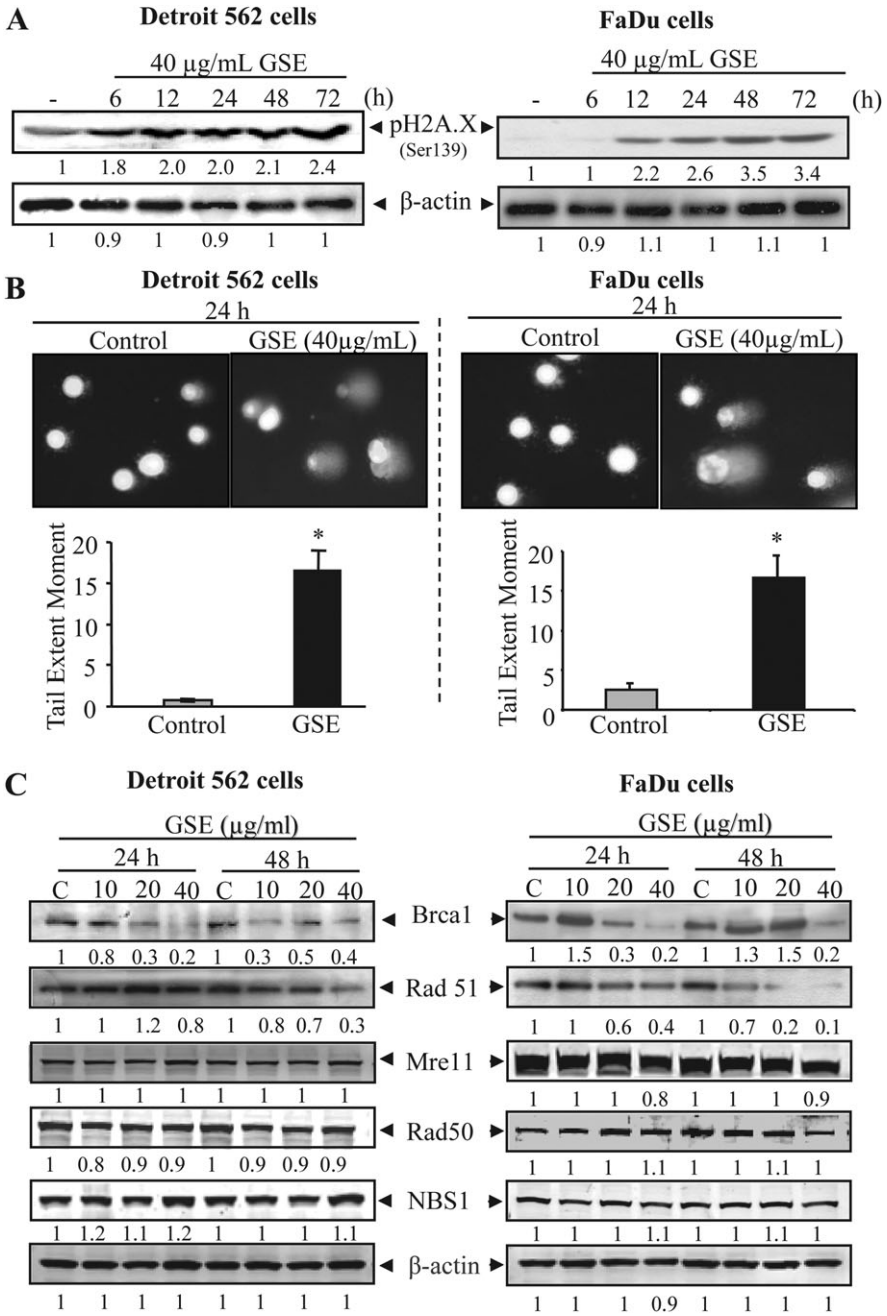

Fig. 3. Effect of GSE on DNA damage and DNA damage repair molecules in HNSCC cells. (**A**) Detroit 562 and FaDu cells were treated with either dimethyl sulfoxide or GSE (40 µg/ml) for 6–72 h. Total cell lysates were prepared and analyzed for phospho-H2A.X (Ser139). (**B**) Comet assay was performed in Detroit 562 and FaDu cells after 24 h of GSE treatment (40 µg/ml), tail extent moment was measured and photomicrographs were captured at ×200 as described in 'Materials and methods'. Each bar is representative of mean ± SEM of three samples for each treatment. $^{*}P < 0.001$ (**C**) Detroit 562 and FaDu cells were treated with GSE (40 µg/ml) for 24 and 48 h and total cell lysates were analyzed for the expression of DNA damage repair molecules Brca1, Rad51, Mre11, Rad50 and Nbs1. (A and C) Equal protein loading was confirmed by reprobing the membrane with β-actin after stripping. The densitometry data below the bands represent fold change as compared with vehicle control after normalization with respective loading control.

in both HNSCC cell lines. We did not, however, find any noticeable effect of GSE treatment on the levels of Rad50, Mre11 and Nbs1 involved in NHEJ DNA repair pathway (Figure 3C). Together, these results show that GSE causes irreparable DNA damage in HNSCC cells in part due to a strong decrease in repair enzymes, Brca1 and Rad51.

GSE induces subnuclear phosho-H2A.X foci formation without the formation of Rad51 and Brca1 repair foci in HNSCC cells

DSBs repair involves localization of repair enzymes at the site of DNA damage, and the active DNA repair is indicated by the formation of subnuclear foci of Rad51 and Brca1 (30). Accordingly, we next examined whether GSE affects the formation of the subnuclear foci in both Detroit 562 and FaDu cells by immunofluorescence. As shown in Figure 4A, GSE treatment (40 μg/ml for 24 h) resulted in the formation of prominent H2A.X foci, indicating DNA damage as compared with control cells but it failed to form both Brca1 and Rad51 foci (Figure 4B and 4C). In contrast, mitomycin C (20 ng/ml for 24 h) caused formation of H2A.X foci indicating DNA damage (Figure 4A) but also displayed a dramatic increase in nuclear Rad51 and Brca1 foci formation (Figure 4B and 4C), demonstrating that mitomycin C-mediated DNA damage is restored by activation of DNA repair machinery. This comparison further support that GSE causes DNA damage in HNSCC cells that does not result in the activation of DNA repair machinery.

GSE-induced DNA damage and apoptotic cell death is through an increased intracellular ROS level in HNSCC cells

In recent years, several studies have evaluated the pro-oxidant effects of phytochemicals in cancer cells and have demonstrated that their biological effects could be through an enhanced intracellular ROS level (32,33). Therefore, based on our data shown in Figures 1–4, we next investigated whether GSE increases the production of intracellular ROS in HNSCC cells. As shown in Figure 5A, GSE (40 μg/ml) treatment increased the ROS production after 3 and 6 h in both Detroit 562 and FaDu cells measured using DCF-DA and DHE fluorescent dyes as detailed in Materials and methods. To further confirm the pro-oxidant effects of GSE, we pretreated Detroit 562 and FaDu cells with free radical-scavenging agent, NAC and as shown in Figure 5B, NAC pretreatment completely reversed the GSE-induced intracellular ROS formation in both cell lines as indicated by DCF-DA and DHE staining, and NAC alone decreased the basal level of ROS in both of the HNSCC cells. Next, we examined whether the GSE-induced ROS are primarily responsible for DNA damage as well as for the resultant cell death. As shown in Figure 5C, NAC pretreatment significantly reversed the GSE (40 μg/ml) effect on cell viability and cell death in both Detroit 562 and FaDu cells. It should be noted that in the absence of GSE, NAC (5 and 15 mM in Detroit 562 and FaDu cells, respectively) alone did not show any toxicity to the cells for the given time period (3–24 h). In addition, NAC pretreatment also reversed the GSE-induced levels of phosphorylated H2A.X and cleaved caspase 3 in both HNSCC cell lines (Figure 5D), suggesting the potential role of ROS in GSE-induced DNA damage and apoptosis. However, NAC pretreatment was not able to reinstate GSE-mediated decrease in protein expression of Brca1 and Rad51 in both HNSCC cell lines (data not shown), indicating the possible involvement of an alternative mechanism, which needs to be examined in future. Together, these results clearly suggest the role of ROS in GSE-induced DNA damage as well as apoptosis in HNSCC cells.

GSE suppresses HNSCC cells xenograft growth in nude mice

Next, we evaluated GSE effect on the growth of Detroit 562 and FaDu cells xenografts in nude mice and found that consistent with our *in vitro* results, GSE feeding strongly inhibits the growth of HNSCC xenograft tumors in a time-dependent manner (Figure 6A and 6B). Overall, at the end of the study, animals from GSE-fed group had ∼67% ($P < 0.05$) and 65% ($P < 0.001$) lesser tumor volume and 70% ($P < 0.001$) and 55% ($P < 0.001$) lesser tumor weight in Detroit 562 and FaDu xenografts, respectively (Figure 6A and 6B). There was no significant change in the diet consumption and body weight gain between control and GSE-fed animal groups (data not shown). Next, xenografts were fixed and embedded in paraffin and a histopathological analysis was performed by hematoxylin and eosin staining, where we found strong necrotic tissue in GSE-fed Detroit 562 xenograft tissues compared with control (data not shown). This limited its use for IHC studies, and therefore tissues only from FaDu xenografts were processed for IHC analyses.

Effect of GSE on proliferation, apoptosis and DNA damage biomarkers in FaDu xenografts

To further support our cell culture findings, next we analyzed the xenograft tissues for PCNA, TUNEL and p-H2A.X (Ser139), biomarkers for proliferation, apoptosis and DNA damage, respectively. As shown in Figure 6C, compared with controls, FaDu xenograft tissues from GSE-fed group showed decreased PCNA-positive cells (37%, $P < 0.001$), 3.9-fold increase ($P < 0.001$) in TUNEL-positive cells and most profoundly, a 19-fold increase in phospho-H2A.X (Ser139)-positive cells. Together, these results suggested that GSE exhibits strong antiproliferative, pro-apoptotic and DNA-damaging effects both *in vitro* and *in vivo* as a part of its efficacy against HNSCC cells.

Discussion

HNSCC is one of the major public health problems worldwide including the USA (1). Though the curability of disease if diagnosed at early stage is high, most of the patients are diagnosed at relatively advanced stage, and hence the survival of advanced HNSCC patients is poor. In the past, different combination treatment approaches have been evaluated against HNSCC but with limited success (34). Multiple lines of evidences suggest that the dietary components from vegetables and fruits provide significant protection against oral cancer (35,36). Our results in the present study showed that dietary supplement GSE triggers DNA damage through an accumulation of intracellular ROS and decrease in DNA repair enzymes, leading to cell cycle arrest and apoptotic cell death in human HNSCC cells in culture. Similar results, to cell culture, were also observed in nude mice xenograft studies showing strong GSE efficacy in inhibiting human HNSCC tumor growth, which involved antiproliferative, pro-apoptotic and DNA-damaging effects *in vivo* as well.

The cell cycle in cancer cells is deregulated due to abnormal expression of cyclins and cyclin-dependent kinases (37). Therefore, targeting the uncontrolled cell cycle progression in tumor cells through modulating the cyclins/cyclin-dependent kinases expression as well as phosphatases regulating their function could be a promising approach to manage excessive cancer cell proliferation (28,37). Results from the present study revealed that GSE decreases cyclin B1 expression along with increase in Cdc25C phosphorylation and inactivation leading to cell cycle arrest in HNSCC cells. Furthermore, progression of cells through different phases of cell cycle are tightly regulated by Chk1 and Chk2, which deter cells to enter into new phase without the successful completion of the earlier phase (38,39). In general, Chk1 and Chk2 play a central role in transducing oxidative stress and DNA damage signal from ATM/ATR, and these kinases are largely inactive in cancer cells (38,39). Results from present study suggest that GSE activates DNA damage sensors and cellular Chks leading to phosphorylation and inactivation of Cdc25C and resulting in cell cycle arrest.

The overexpression of DNA repair genes has been correlated with decreased survival in patients with prostate, lung, breast and head and neck cancer (40–42). Therefore, targeting DNA repair pathways along with DNA damage induction may provide an efficient therapy options against cancer progression. Results from present study showed that GSE induces DNA damage specifically the DSBs as evident by increased H2A.X phosphorylation. DSBs are usually repaired through one of the two mechanisms, NHEJ or HRR. In NHEJ, DNA ligase IV, DNA-PKCs, Brca1, XRCC4, Rad50/Mre11/Nbs1, Ku70/Ku80 types of enzymes utilize pieces of DNA adjacent to the break to join and fill

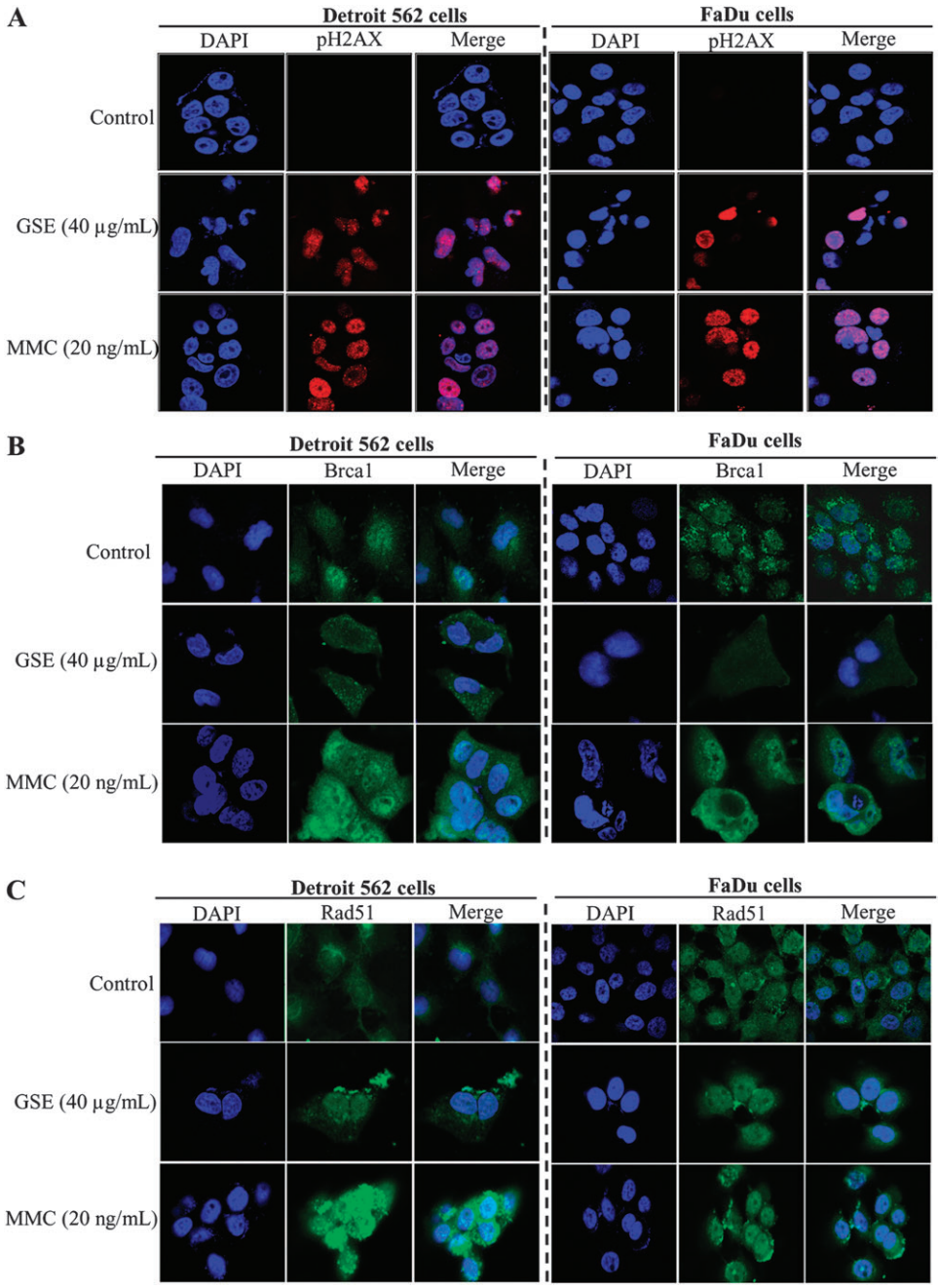

Fig. 4. Effect of GSE on phospho-H2A.X, Brca1 and Rad51 foci formation in HNSCC cells. Detroit 562 and FaDu cells were treated with GSE (40 µg/ml) for 24 h and then probed with specific primary antibodies for (**A**) phospho-H2A.X (Ser139), (**B**) Brca1 and (**C**) Rad51 as detailed in 'Materials and methods'. Thereafter, cells were incubated with fluorescein isothiocyanate-tagged secondary antibodies and counterstained with 4′,6′-diamidino-2-phenylindole (DAPI). Cells were finally visualized under Nikon D eclipse C1 confocal microscope and images were processed using EZ-C1 Free-viewer software. Data, representative of experiment done in triplicate, show the subnuclear foci formation for phospho-H2A.X, Brca1 and Rad51 after GSE treatment. Mitomycin C (20 ng/ml for 24 h)-treated cells were used as positive control.

in the ends (30). In contrast, during HRR the homologous chromosome serves as a template for repair and involves enzymes, including Brca1, Rad51 and/or Brca2 and takes place in late S- and G_2-phases of the cell cycle (43). Interestingly, GSE treatment resulted in G_2/M arrest in HNSCC cells, thereby providing an ideal condition for DNA repair mainly through HRR. But GSE also decreased the levels of Brca1 and Rad51, involved in HRR pathway, thereby inhibiting any repair of the damaged DNA. These results suggest that the GSE-induced downregulation of DNA repair pathways may in part be responsible for high sensitivity of HNSCC cells toward the cytotoxic effects of GSE following ROS generation and associated DNA damage.

In general, ROS are generated in the cell as the byproduct of cellular metabolism and their role have been described in several diseases including cancer (44). However, ROS are like double-edged sword and when their intracellular levels overwhelm the cellular antioxidant capacity, it could be detrimental to cells survival (44,45). Considering the potential role of ROS in inducing DNA damage and apoptosis in cancer cells, the proposed strategy relevant for cancer treatment would be to increase intracellular ROS in cancer cells to toxic level that causes oxidative stress, inactivates redox-signaling molecules and induce cell death (44). Importantly, such an approach will adversely affect only the cancer cells as they have higher ROS level compared with normal cells (45). In line to this strategy, we have shown that GSE increases

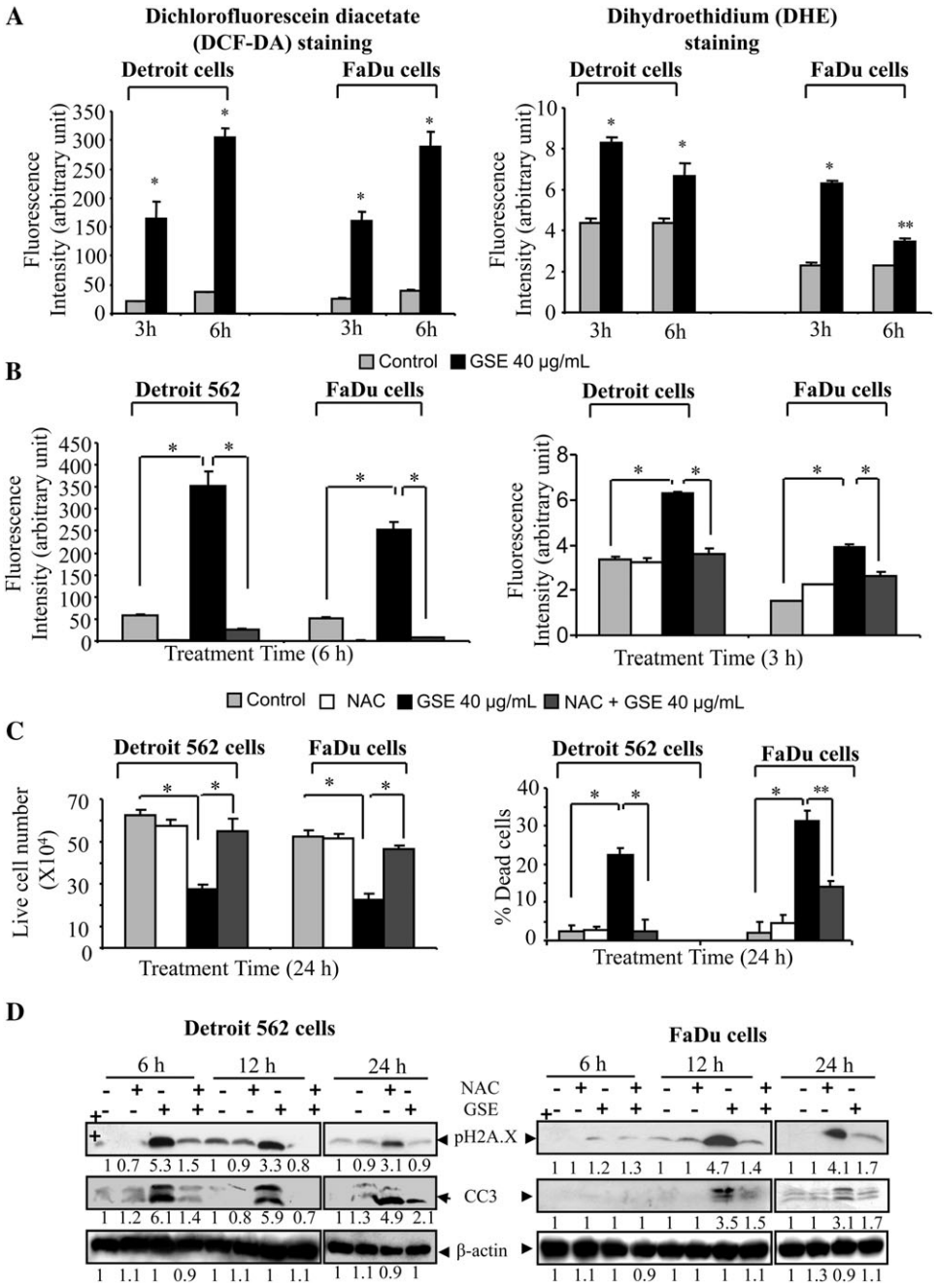

Fig. 5. Effect of GSE on intracellular ROS levels and their role in biological efficacy of GSE in HNSCC cells. (**A**) Detroit 562 and FaDu cells were treated with 20 µM of DCF-DA or 10 µM of DHE in dark, followed by GSE (40 µg/ml), and DCF-DA fluorescence intensity was measured using fluorescence plate reader and DHE intensity was analyzed using flow cytometry as described in the 'Materials and methods'. (**B**) NAC (5 mM for Detroit 562 and 15 mM for FaDu cells) was added 15 min prior to GSE and cells were processed after 6 h (DCF-DA) and 3 h (DHE) for measuring the ROS level. (**C** and **D**) Detroit 562 and FaDu cells were pretreated with NAC for 15 min followed by 40 µg/ml of GSE. Experiment was terminated after 24 h and cell number and cell death were determined. Under similar experimental conditions, total cell lysates were prepared after 6, 12 and 24 h and analyzed for phospho-H2A.X (Ser139) and cleaved caspase 3 levels. The data shown in (A–C) are representative of mean ± SEM of three samples for each treatment. $^{*}P < 0.001$; $^{**}P < 0.05$. The immunoblots were stripped and reprobed with β-actin to ensure equal protein loading. The densitometry values represent fold change as compared with vehicle control after normalization with respective loading control.

intracellular ROS, triggers DNA damage and G_2/M arrest, leading to cell death. Our result also showed that pretreatment of HNSCC cells with NAC substantially decreased GSE-induced intracellular ROS, cell number and cell death, DNA damage and apoptosis. However, the exact mechanism responsible for GSE-caused increase in intracellular ROS level needs further investigations in future studies.

Recent studies have shown that in response to a death stimulus, there is often a continuum of apoptosis and necrosis (46). Many chemotherapeutic drugs could induce apoptosis at lower doses and necrotic death at higher doses. Similar to apoptosis, necrosis is a complicated phenomenon involving several inter-related and cross-regulated events, such as mitochondrial depolarization, depletion of intracellular adenosine triphosphate, disturbance of calcium homeostasis, PARP activation, activation of non-apoptotic proteases, ROS generation and disruption of the plasma membrane (46). In the present study, we observed apoptotic death induction by GSE in both the HNSCC cell lines (Detroit 562 and FaDu cells) in cell culture, but surprisingly we observed a tumor-specific necrosis in Detroit 562 xenografts with GSE feeding. Since

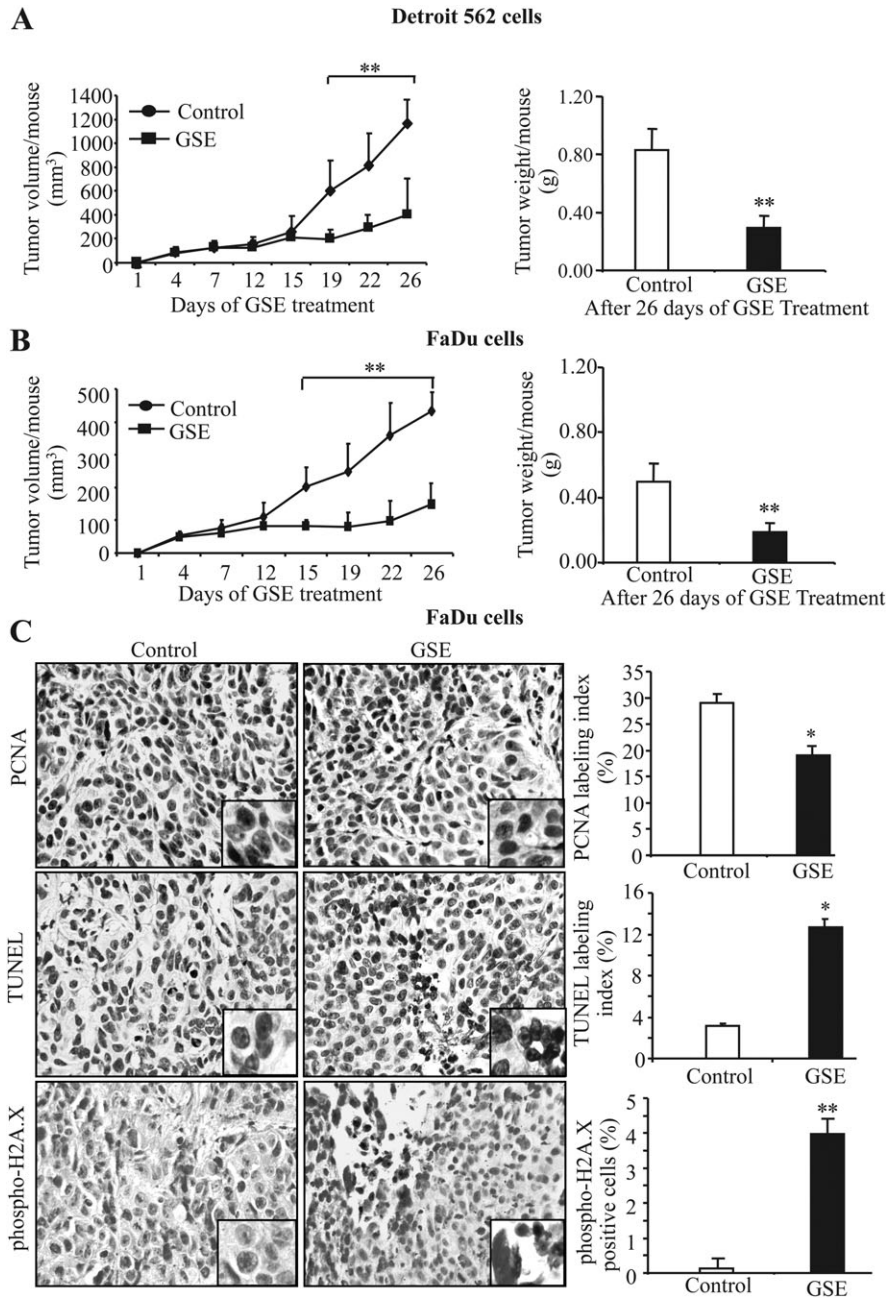

Fig. 6. Effect of dietary feeding of GSE on HNSCC Detroit 562 and FaDu tumor xenograft growth in athymic nude mice along with *in vivo* proliferation, apoptosis and DNA damage. Nude mice were injected with Detroit 562 or FaDu cells, fed with 0.2% GSE (wt/wt) in diet and animals analyzed for (**A**) tumor volume (in mm^3) and (**B**) tumor weight as mentioned in Material and methods. The data shown are average tumor volume ± SEM of seven mice per group. (**C**) FaDu xenograft tissue samples from both control and GSE-fed groups were subjected to IHC analysis, and representative photographs are shown for PCNA-, TUNEL- and phospho-H2A.X (Ser139)-positive cells at ×400 magnification. The quantitative data shown are mean ± SEM of five individual tumor samples from each group. $^{*}P < 0.001$; $^{**}P < 0.05$.

tumor tissues were analyzed only at the end of the study i.e. after 26 days of GSE feeding, we could not conclude whether the observed cell death in Detroit 562 xenografts is primarily a necrotic event or is the result of secondary necrosis of apoptotic cells. Since we observed necrosis only *in vivo*, it could also be the result of strong antiangiogenic effect of GSE causing nutrient deprivation and reduced oxygen supply to the tumor cells. Furthermore, we cannot rule out the possibility that the necrosis induction in Detroit 562 cells is a cell line-specific effect of GSE which could be due to specific genetic differences within this cell line as compared with FaDu and possibly other HNSCC cell lines. Therefore, future multiple time-point studies focusing on necrotic cell death mechanisms especially in immunocompetent mice might reveal definite details regarding GSE-induced cell death in HNSCC cells.

In terms of its toxicity and bioavailability, *in vivo* studies with GSE have shown that it is well tolerated and is considered safe as dietary supplement for human consumption (47,48). In acute oral toxicity evaluation of grape seed proanthocyanidin extract, lethal dose 50 was found to be >5000 mg/kg with single oral dose via gastric intubation to fasting male and female albino rats (47). In chronic toxicity studies, administration of 100, 250 or 500 mg/kg per day of GSE for 6 months to female B6C3F1 mice did not cause any detrimental effects (47). In other 90 day oral toxicity studies with GSE (up to 2%

in diet) in rats, no significant toxicological effects were observed (21,48). Furthermore, GSE did not show any genotoxic effect in chromosomal aberration test using Chinese hamster lung cells and sister chromatid exchange using human lymphocytes (48,49). Earlier, Sano *et al.* (50) have reported that procyanidin B1 could be detected in human serum 2 h after the consumption of 2 g of GSE by healthy adults confirming the bioavailability of one of the active constituent of GSE. The GSE dose used in the present study (0.2% in diet) equates to ∼300 mg/kg daily dose, and as per Hoh *et al.* (51) criterion, this dose extrapolates to ∼1.8 g GSE/person daily, assuming a body surface area of 1.8 m^2 accompanying a body weight of 70 kg. Therefore, anticancer efficacy of GSE reported in the present study could be translated in HNSCC patients without any toxicity.

In summary, the present study clearly demonstrated GSE efficacy against HNSCC cells both in cell culture and animal models. Mechanistic studies suggested that GSE causes irreparable DNA damage via enhancing intracellular ROS level, leading to cell cycle arrest and apoptotic cell death. Considering the limited therapeutic options available against HNSCC, results from the present study support additional studies investigating GSE efficacy against HNSCC both in chemoprevention and intervention protocols and define the mechanisms of its efficacy. This would help support the translational potential of GSE in controlling HNSCC.

Funding

This work was supported by the R01 grants AT003623 from the National Center for Complementary and Alternative Medicine and CA91883 from the National Cancer Institute, National Institutes of Health.

Conflict of Interest Statement: None declared.

References

1. Jemal,A. *et al*. (2010) Cancer statistics. *CA Cancer J. Clin.*, **60**, 277–300.
2. Haddad,R.I. *et al*. (2008) Recent advances in head and neck cancer. *N. Engl. J. Med.*, **359**, 1143–1154.
3. Pai,S.I. *et al*. (2009) Molecular pathology of head and neck cancer: implications for diagnosis, prognosis, and treatment. *Annu. Rev. Pathol.*, **4**, 49–70.
4. Silva,S.D. *et al*. (2011) Advances and applications of oral cancer basic research. *Oral Oncol.*, **47**, 783–791.
5. Leemans,C.R. *et al*. (2011) The molecular biology of head and neck cancer. *Nat. Rev. Cancer*, **11**, 9–22.
6. Leon,X. *et al*. (2005) Metachronous second primary tumours in the aerodigestive tract in patients with early stage head and neck squamous cell carcinomas. *Eur. Arch. Otorhinolaryngol.*, **262**, 905–909.
7. Tan,A.C. *et al*. (2011) Molecular pathways for cancer chemoprevention by dietary phytochemicals. *Nutr. Cancer*, **63**, 495–505.
8. Weng,C.J. *et al*. (2012) Chemopreventive effects of dietary phytochemicals against cancer invasion and metastasis: phenolic acids, monophenol, polyphenol, and their derivatives. *Cancer Treat. Rev.*, **38**, 76–87.
9. Pan,M.H. *et al*. (2011) Molecular mechanisms for chemoprevention of colorectal cancer by natural dietary compounds. *Mol. Nutr. Food Res.*, **55**, 32–45.
10. Tyagi,A. *et al*. (2011) Resveratrol selectively induces DNA damage, independent of Smad4 expression, in its efficacy against human head and neck squamous cell carcinoma. *Clin. Cancer Res.*, **17**, 5402–5411.
11. Cooke,D. *et al*. (2005) Anthocyans from fruits and vegetables—does bright colour signal cancer chemopreventive activity? *Eur. J. Cancer*, **41**, 1931–1940.
12. Gullett,N.P. *et al*. (2010) Cancer prevention with natural compounds. *Semin. Oncol.*, **37**, 258–281.
13. Weber,H.A. *et al*. (2007) Comparison of proanthocyanidins in commercial antioxidants: grape seed and pine bark extracts. *J. Agric. Food Chem.*, **55**, 148–156.
14. Veluri,R. *et al*. (2006) Fractionation of grape seed extract and identification of gallic acid as one of the major active constituents causing growth inhibition and apoptotic death of DU145 human prostate carcinoma cells. *Carcinogenesis*, **27**, 1445–1453.
15. Kaur,M. *et al*. (2009) Anticancer and cancer chemopreventive potential of grape seed extract and other grape-based products. *J. Nutr.*, **139**, 1806S–1812S.
16. Velmurugan,B. *et al*. (2008) Inhibition of azoxymethane-induced colonic aberrant crypt foci formation by silibinin in male Fisher 344 rats. *Cancer Prev. Res. (Phila)*, **1**, 376–384.
17. Bagchi,D. *et al*. (2000) Free radicals and grape seed proanthocyanidin extract: importance in human health and disease prevention. *Toxicology*, **148**, 187–197.
18. Kar,P. *et al*. (2009) Effects of grape seed extract in Type 2 diabetic subjects at high cardiovascular risk: a double blind randomized placebo controlled trial examining metabolic markers, vascular tone, inflammation, oxidative stress and insulin sensitivity. *Diabet. Med.*, **26**, 526–531.
19. Shirataki,Y. *et al*. (2000) Selective cytotoxic activity of grape peel and seed extracts against oral tumor cell lines. *Anticancer Res.*, **20**, 423–426.
20. King,M. *et al*. (2007) Oral squamous cell carcinoma proliferative phenotype is modulated by proanthocyanidins: a potential prevention and treatment alternative for oral cancer. *BMC Complement. Altern. Med.*, **7**, 22.
21. Wren,A.F. *et al*. (2002) 90-day oral toxicity study of a grape seed extract (IH636) in rats. *J. Agric. Food Chem.*, **50**, 2180–2192.
22. Kaur,M. *et al*. (2008) Grape seed extract induces cell cycle arrest and apoptosis in human colon carcinoma cells. *Nutr. Cancer*, **60** (suppl. 1), 2–11.
23. Tice,R.R. *et al*. (2000) Single cell gel/comet assay: guidelines for *in vitro* and *in vivo* genetic toxicology testing. *Environ. Mol. Mutagen.*, **35**, 206–221.
24. Deep,G. *et al*. (2008) Isosilybin B causes androgen receptor degradation in human prostate carcinoma cells via PI3K-Akt-Mdm2-mediated pathway. *Oncogene*, **27**, 3986–3998.
25. Singh,R.P. *et al*. (2009) Silibinin suppresses growth of human prostate carcinoma PC-3 orthotopic xenograft via activation of extracellular signal-regulated kinase 1/2 and inhibition of signal transducers and activators of transcription signaling. *Clin. Cancer Res.*, **15**, 613–621.
26. Raina,K. *et al*. (2007) Oral grape seed extract inhibits prostate tumor growth and progression in TRAMP mice. *Cancer Res.*, **67**, 5976–5982.
27. Chen,Y. *et al*. (2004) Chk1 in the DNA damage response: conserved roles from yeasts to mammals. *DNA Repair (Amst.)*, **3**, 1025–1032.
28. Lagarrigue,S. *et al*. (2011) [Emerging key role of cell cycle regulators in cell metabolism]. *Med. Sci. (Paris)*, **27**, 508–513.
29. Cory,S. *et al*. (2002) The Bcl2 family: regulators of the cellular life-or-death switch. *Nat. Rev. Cancer*, **2**, 647–656.
30. O'Neil,N. *et al*. (2006) DNA repair. *WormBook*, 1–12.
31. O'Driscoll,M. *et al*. (2006) The role of double-strand break repair—insights from human genetics. *Nat. Rev. Genet.*, **7**, 45–54.
32. Kaur,M. *et al*. (2011) Grape seed extract upregulates p21 (Cip1) through redox-mediated activation of ERK1/2 and posttranscriptional regulation leading to cell cycle arrest in colon carcinoma HT29 cells. *Mol. Carcinog.*, **50**, 553–562.
33. Low,I.C. *et al*. (2010) Bcl-2 modulates resveratrol-induced ROS production by regulating mitochondrial respiration in tumor cells. *Antioxid. Redox Signal.*, **13**, 807–819.
34. Datema,F.R. *et al*. (2010) Impact of comorbidity on short-term mortality and overall survival of head and neck cancer patients. *Head Neck*, **32**, 728–736.
35. Conway,D.I. (2007) Each portion of fruit or vegetable consumed halves the risk of oral cancer. *Evid. Based Dent.*, **8**, 19–20.
36. Pavia,M. *et al*. (2006) Association between fruit and vegetable consumption and oral cancer: a meta-analysis of observational studies. *Am. J. Clin. Nutr.*, **83**, 1126–1134.
37. Musgrove,E.A. *et al*. (2011) Cyclin D as a therapeutic target in cancer. *Nat. Rev. Cancer*, **11**, 558–572.
38. M. Molinari. (2000) Cell cycle checkpoints and their inactivation in human cancer. *Cell Prolif.*, **33**, 261–274.
39. Hartwell,L.H. *et al*. (1989) Checkpoints: controls that ensure the order of cell cycle events. *Science*, **246**, 629–634.
40. Connell,P.P. *et al*. (2006) Pilot study examining tumor expression of RAD51 and clinical outcomes in human head cancers. *Int. J. Oncol.*, **28**, 1113–1119.
41. Mitra,A. *et al*. (2009) Overexpression of RAD51 occurs in aggressive prostatic cancer. *Histopathology*, **55**, 696–704.
42. Maacke,H. *et al*. (2000) Over-expression of wild-type Rad51 correlates with histological grading of invasive ductal breast cancer. *Int. J. Cancer*, **88**, 907–913.
43. Helleday,T. *et al*. (2007) DNA double-strand break repair: from mechanistic understanding to cancer treatment. *DNA Repair (Amst.)*, **6**, 923–935.
44. Circu,M.L. *et al*. (2010) Reactive oxygen species, cellular redox systems, and apoptosis. *Free Radic. Biol. Med.*, **48**, 749–762.
45. Schumacker,P.T. (2006) Reactive oxygen species in cancer cells: live by the sword, die by the sword. *Cancer Cell*, **10**, 175–176.

46. Zong,W.X. *et al*. (2006) Necrotic death as a cell fate. *Genes Dev.*, **20**, 1–15.
47. Ray,S. *et al*. (2001) Acute and long-term safety evaluation of a novel IH636 grape seed proanthocyanidin extract. *Res. Commun. Mol. Pathol. Pharmacol.*, **109**, 165–197.
48. Yamakoshi,J. *et al*. (2002) Safety evaluation of proanthocyanidin-rich extract from grape seeds. *Food Chem. Toxicol.*, **40**, 599–607.
49. Popp,R. *et al*. (1991) Induction of sister-chromatid exchanges (SCE), polyploidy, and micronuclei by plant flavonoids in human lymphocyte cultures. A comparative study of 19 flavonoids. *Mutat. Res.*, **246**, 205–213.
50. Sano,A. *et al*. (2003) Procyanidin B1 is detected in human serum after intake of proanthocyanidin-rich grape seed extract. *Biosci. Biotechnol. Biochem.*, **67**, 1140–1143.
51. Hoh,C. *et al*. (2006) Pilot study of oral silibinin, a putative chemopreventive agent, in colorectal cancer patients: silibinin levels in plasma, colorectum, and liver and their pharmacodynamic consequences. *Clin. Cancer Res.*, **12**, 2944–2950.

Received December 6, 2011; revised January 9, 2012;
accepted January 15, 2012